Vascular Endothelial Growth Factor Ameliorated Palmitate Induced Cardiomyocyte Injury via JNK Pathway

Shiya Wang
First Affiliated Hospital of Soochow University
Cao Zou
First Affiliated Hospital of Soochow University
Xiaofeng Liu
Hai'an People's Hospital
Yonjin Yan
Hai'an People's Hospital
Shunzhon Gu
Hai'an People's Hospital
Qinghua Wang
Comparative medicine institution of Nantong University
Xun Li (xunli58@126.com)
First Affiliated Hospital of Soochow University

Research Article

Keywords: PAL, VEGF, cardiomyocyte, apoptosis, MAPK, caspase 3, NF-κB

Posted Date: December 29th, 2020

DOI: https://doi.org/10.21203/rs.3.rs-120750/v1

Version of Record: A version of this preprint was published at In Vitro Cellular & Developmental Biology - Animal on November 17th, 2021. See the published version at https://doi.org/10.1007/s11626-021-00616-z.

Abstract

Objective To investigate the effect of palmitate (PAL) on apoptosis and the timing and activity of VEGF expression in HHHM2 myocardial cells (a human embryonic cardiomyocyte cell- line).

Methods 1. Cardiomyocytes were divided into the following five groups: the control group and the 0.2 mM, 0.5 mM, 0.8 mM, and 1.2 mM PAL groups. We examined the changes in cell viability by MTT assay after PAL incubation for 24 h and the cardiomyocyte apoptosis rate by FACS examination, and thus determined the effective concentration of PAL. The transcription levels of *CASP3*, *Bcl-2*, *Bax*, and *VEGF* were detected by quantitative fluorescence PCR and the protein expression of caspase 3 and VEGF by western blot.

2. To observe the time-dependent effects on cell injury induced by 0.5 mM PAL, cardiomyocytes were divided into 0, 4, 8, 16, 24, and 48 h groups. The variation in cell viability was examined by MTT assay. The transcription levels of *CASP3*, *Bcl-2*, *Bax*, and *VEGF* were detected by quantitative fluorescence PCR and the protein expression of caspase 3 and VEGF by western blot.

3. To observe the effects of VEGF on the PAL induced apoptosis of cardiomyocytes, the cells were divided into the control group and the VEGF overexpression group. At 24 h after transfection, cells were incubated with 0.5 mM PAL for 6, 12, 24, and 48 h. Cell viability was examined by MTT assay. The apoptosis rate was measured by FACS using the Annexin V-FITC kit. The transcription levels of *CASP3*, *Bcl-2*, *Bax*, *NF-kB p65*, and *VEGF* were measured by quantitative fluorescence PCR, the protein expression of VEGF, caspase 3, Bcl-2, Bax, NF-κB p65, p-JNK/JNK, and p-ERK/ERK were measured by western blot, as well as caspase 3 activity.

Results 1. A dose-dependent relation between the concentration of PAL and H9c2 cardiomyocyte injury was observed. In the 0.5 mM group, the apoptosis rate was increased significantly, while cell viability was decreased, indicating that 0.5 mM PAL was the ideal concentration to induce cardiomyocyte apoptosis. The expression of caspase 3 and Bax was significantly increased, and the expression of VEGF was enhanced, while the levels of Bcl-2 remained unchanged during the process.

2. A significant time-dependent relation between PAL and cardiomyocyte injury was observed. The apoptosis rate was increased greatly after 16 h treatment with 0.5 mM PAL.

3. Cell viability was restored by VEGF overexpression during treatment with 0.5 mM PAL. The apoptosis rate was also reduced by VEGF overexpression, as detected by FACS. The expression of caspase 3, Bax, and NF-κB p65 was significantly decreased, Bcl-2 and VEGF expression was dramatically increased, p-JNK/JNK expression was significantly enhanced, p-ERK/ERK levels did not exhibit a significant change, and the activity of caspase 3 was significantly decreased.

Conclusions 1. PAL can induce injury and apoptosis in HHHM2 myocardial cells, and these effects are time-dependent. A PAL concentration of 0.5 mM was ideal to establish the cardiac cell injury model.

2. PAL at a concentration of 0.5 mM can effectively induce cardiomyocyte injury and enhance the expression of caspase 3, Bax, and VEGF, especially after 24 h and 48 h of PAL treatment.

3. VEGF overexpression can reverse the effects of PAL on apoptosis and cell viability. In addition, VEGF overexpression inhibited the expression of proapoptotic and inflammatory factors, caspase 3 activity, and transduction of the MAPK signaling pathway.

Research Highlights

► Palmitate can induce an HHHM2 cell injury model

► VEGF expression was activated under palmitate stimulation

► VEGF overexpression ameliorated HHHM2 cell injury

► The JNK pathway was involved in HHHM2 cell injury

Introduction

Recent studies support the hypothesis that cardiomyocytes harbor no ability of self-renewal and replication, for they are terminally differentiated cells (1). Thus, it is believed that the damage and apoptosis of cardiomyocytes are mainly ascribed to cell necrosis (2). However, the latest research shows that cardiomyocyte apoptosis is also an important biological basis for the normal physiological function of the heart (1). The rapid changes in the human diet, and the concomitant increase in human fat deposition, have led to a high incidence of obesity, diabetes, and cardiovascular diseases (3). Increases in serum lipid levels result in damage to and irritation of the cardiovascular system; particularly, ectopic fat deposition places an additional burden on the heart, which can lead to myocardial injury (4). Energy supply to the adult heart mainly relies on fatty acids; abnormal fatty acid metabolism is often accompanied with heart disease or systemic disease (5,6). It has been reported that acute myocardial ischemia, diabetes, and obesity patients have an increased risk of abnormal deposition of myocardial fat, leading to heart failure (7).

Palmitate (PAL), a saturated fatty acid, has been shown to accumulate in cardiomyocytes, vascular smooth muscle cells, hepatic cells, and islet beta cells (8–12). PAL accumulation in cardiomyocytes can lead to “lipotoxicity” and thus result in cardiomyocyte injury, apoptosis, and heart dysfunction and failure (3,13–15). Transgenic mouse models with abnormal lipid accumulation in the heart demonstrated that an imbalance of lipid uptake and utilization in cardiomyocytes led to apoptosis and contributed to cardiomyopathy (16,17). PAL was also found to induce apoptosis in a variety of cells in vitro; however, the exact molecular and cellular mechanisms by which fatty acids cause apoptosis remain unclear.

Vascular endothelial growth factor (VEGF), also known as vascular osmotic factor, is a member of the vascular endothelial growth factor family and exerts multiple physiological effects, including

proangiogenesis effects, blood vessel dilation, increasing vascular permeability, and promoting cell proliferation, differentiation, and viability. Extensive studies show its role in the fields of diabetes, rheumatoid arthritis, kidney disease, cardiovascular disease, tumor, and central nervous system diseases (18–20). VEGF induced migration and proliferation of vascular endothelial cells in the process of angiogenesis and promoted the secretion of protease and fibrinogen activator, which stimulated the cells to escape from the matrix by degrading the vascular basement membrane (21). Platelet-derived growth factors (PDGFs) are secreted by endothelial cells under the stimulation of VEGF, thus maintaining vascular homeostasis (22). VEGF-A, one of the five members in the VEGF family, shows the highest specificity and the strongest physiological effects (23,24). VEGF directly interacts with mitogens in endothelial cells and thus promotes the permeability of blood vessels, increases blood oxygen supply, and enhances the proliferation of vascular endothelial cells (25,26). Inhibition of extracellular signal regulated kinase (ERK)–MAPK signaling by PD98059 significantly increased cardiomyocyte apoptosis, caspase 3 activity, and the myocardial defect area, and the effects on apoptosis could be reversed by the administration of fasudil (a Rho kinase inhibitor) [38]. The ERK–MAPK pathway promotes the remodeling of myocardial cell morphology in glucocorticoid induced cardiomyocyte injury [40].

In this study, we (i) observed the effects of VEGF overexpression on myocardial apoptosis in a PAL induced cardiomyocyte apoptosis model and (ii) detected the changes of the MAPK pathway, in order to explore the mechanisms and protective factors of myocardial apoptosis injury at the cellular and molecular levels.

Materials And Methods

Cell culture and treatments

HHHM2 cardiomyocytes (a human embryonic cardiomyocyte cell line, Lot: JN-B1400) were obtained from Shanghai Jining Shiye Company (Shanghai, China) and cultured in Minimum Essential Medium with Earle's Balanced Salts with 10% fetal bovine serum (Gibco, Rockville, MD, USA) in a bio-incubator at 5% CO_2 and 37 °C (Thermo Fisher Scientific, Waltham, MA, USA). Cells were seeded in a 24-well plate and treated when the confluence reached 50%. Cells were treated with different concentrations of PAL (Sigma-Aldrich, St. Louis, MO, USA) at final concentrations of 0.2, 0.5, 0.8, and 1.2 mM. In the time-course experiments, cells were treated with PAL at a final concentration of 0.5 mM for 0, 4, 8, 16, 24, and 48 h. The pcDNA3.1-VEGFA plasmid was gifted by Dr. Jun Cao's lab at Nantong University. Cells were transfected with VEGFA plasmid according to the manufacturer's instructions.

MTT assay

Cell viability was detected by MTT assay. In brief, cells were seeded into 96-well plates at about 6×10^3 cells/well, and 0.1 mg MTT (Sigma-Aldrich) was added to each well. The whole plate was incubated for 4 h at 37 °C away from light. Then the medium was aspirated and 150 μL dimethyl sulfoxide (DMSO, Sigma-Aldrich) was dropped into each well. After incubation on a rotator for 15 min, the absorbance of

the solution of each well was detected at a wavelength of 490 nm using a microplate reader (Thermo Fisher Scientific, Waltham, MA; Varioskan Flash). The cell viability rate was calculated using the following formula:

Viability rate (%) = 100 × (OD value of experimental group/OD value of control group).

HHHM2 cell apoptosis assessment

Exponentially growing cells were plated in 6-well plates at a density of 1×10^5 cells/well. After culture and treatment, cells were trypsinized and resuspended with binding buffer, and the cell density was adjusted to 1×10^5 cells/mL. Each tube containing 100 μL binding buffer was incubated with 5 μL Annexin V-FITC and 5 μL propidium iodide (PI) for 15 min on ice away from light. An additional 400 μL of binding buffer was added and the samples were analyzed on a flow cytometer (FACS, Beckman Coulter, Pasadena, CA). Each sample was measured in triplicate.

qRT-PCR

Total RNA was extracted from HHHM2 cells with TRIzol reagent (Invitrogen) following the manufacturer's instructions. The RNA was quantified with a spectrophotometer (NanoDrop 2000, Thermo Fisher Scientific) and then reverse-transcribed with PrimeScript™ RT Master Mix (Takara, Shiga Prefecture, Japan, PR036A). Quantitative real-time PCR (qRT-PCR) was performed with SYBR Premix Ex Taq (Tli RNaseH Plus) (Takara, DRR420A). Measurements were carried out in triplicates and data were normalized to endogenous GAPDH expression. Primers were designed by Primer Express software (Applied Biosystems, Foster, CA) and validated. The sequences of primers used are listed in Table 1.

Table 1
Sequences of qRT-PCR primers.

Gene name	Sequence (5' to 3')	Product length
GAPDH	GCAATGTTGCCAGTGTCTGT	86 bp
	GCCTTGACCTTTTCAGCAAG	
CASP3	CAGAGGGGATCGTTGTGAAG	96 bp
	CATACAAAGAAGTCGGCCTCCA	
Bax	GGGATGGCCTCCTTTCCTAC	112 bp
	TTCCAGATGGTGAGTGAGGCA	
Bcl-2	TTCTTTGAGTTCGGTGGGGTC	157 bp
	TGCATATTTGTTTGGGGCAGG	
VEGF	ACTTTCTGCTGTCTTGGATG	127 bp
	CTCGGCTTGTCACATCACCG	
p65	CCCCACGAGCTTGTAGGAAAG	109 bp
	CCAGGTTCTGGAAACTGTGGAT	

The expression of each gene was defined as the fold change compared with the threshold cycle (Ct), and relative expression levels were calculated using the $2^{-\Delta\Delta Ct}$ method by normalization to the housekeeping gene *GAPDH*. Results are presented as the mean from three independent experiments.

Western blot

Cells were harvested at certain time points with pre-cooled phosphate buffered saline (PBS) and washed three times. Cells were in situ incubated with RIPA lysis buffer on ice for 30 min. The lysates were pipetted and centrifuged at 12,000 *g* at 4 °C for 15 min. The supernatant was collected and protein concentrations were determined using a BCA kit. Total protein (20–100 μg per lane) was separated by SDS-PAGE and transferred to a polyvinylidene difluoride (PVDF) membrane (Millipore, Billerica, MA, USA). The membrane was blocked in 5% skim milk solution and incubated with anti-VEGF (ab1316), anti-caspase 3 (ab13847), anti-Bcl-2 (ab692), anti-Bax (ab32503), anti-p65 (ab16502), anti-p-JNK (ab124956), anti-JNK (ab208035), anti-ERK (ab184699), anti-p-ERK (ab201015), or anti-GAPDH (ab181602) at 4 °C overnight. Then membranes were washed and incubated with HRP conjugated secondary antibodies. Protein bands were visualized with ECL Super Signal (Pierce, Rockford, IL, USA). Images were taken using a Tanon 5200 system (Shanghai, China) and analyzed by ImageJ software (NIH, NY, USA), using GAPDH as an internal control.

Statistical analysis

Statistical analysis was performed using SPSS Statistics 24.0 (SPSS Inc., Chicago, IL, USA). All data are presented as mean ± standard deviation (± S), and the time-course data such as those from the MTT

assay were analyzed by the paired Student *t*-test. Differences between groups (0, 24, 48 h) were analyzed using one-way analysis of variance, followed by the Newman–Keuls test, with significance measured at $*P < 0.05$ or $**P < 0.01$.

Results

1. Effects of different palmitate concentrations on cell survival

HHHM2 cells were treated with PAL at final concentrations of 0.2, 0.5, 0.8, and 1.2 mM and collected after 24 h to measure cell viability. Results showed that a slight decrease was observed in the 0.2 mM group, while cell viability was significantly decreased after incubation with 0.5 mM PAL ($P < 0.05$) compared with the control group. A very large decrease in cell viability was found in the 0.8 mM ($P < 0.01$) and 1.2 mM groups ($P < 0.001$). Compared to the 0.2 mM group, cell viability was significantly lower in the 0.8 mM ($P < 0.05$) and 1.2 mM groups ($P < 0.01$), but compared with the 0.5 mM group, no significant difference was observed in the 0.8 mM group ($P > 0.05$) and the 1.2 mM group ($P > 0.05$) (Fig. 1A). These data indicate that PAL successfully influenced myocardial cell viability and functioned in a certain range of concentrations.

2. Effects of different palmitate concentrations on apoptosis

To explore the effects of PAL on HHHM2 cell apoptosis, a range of PAL solutions was selected to stimulate cells for 24 h as described above. The Annexin V/PI apoptosis assay kit was used to detect the changes in apoptosis.

With increasing PAL concentrations, the apoptosis rate of HHHM2 cells also increased gradually. The apoptosis rate in the 0.2 mM group was significantly higher than that in the control group ($P < 0.05$). Simultaneously, the apoptosis rate was significantly higher in the 0.5 mM group compared with the control group ($P < 0.01$) and the 0.2 mM group ($P < 0.05$). In addition, the apoptosis rate was significantly enhanced in the 0.8 mM ($P < 0.01$) and 1.2 mM groups ($P < 0.01$) compared to the control group, while no significant difference was found compared to the 0.5 mM group (Fig. 1B, C).

3. PAL altered the expression of apoptosis related genes

HHHM2 cells were incubated with PAL at final concentrations of 0.2, 0.5, 0.8, and 1.2 mM for 24 h. RNA was collected and gene expression was analyzed. *CASP3* expression was significantly increased in the 0.2 mM group ($P < 0.05$) and the 0.5, 0.8, and 1.2 mM groups compared to the control group ($P < 0.01$). No significant difference in *CASP3* expression was observed in the 0.5 mM group compared to the 0.2 mM group ($P > 0.05$), while *CASP3* expression was significantly higher in the 0.8 and 1.2 mM groups compared with the 0.2 mM group ($P < 0.05$) (Fig. 2A). In addition, expression of *Bax* was enhanced by the stimulation of PAL. The expression level of *Bax* was increased significantly in the 0.2 mM group ($P <$

0.05) and the 0.5, 0.8, and 1.2 mM groups ($P < 0.01$) compared to the control group. Moreover, *Bax* expression was significantly higher in the 0.8 and 1.2 mM groups compared to the 0.5 mM group ($P < 0.05$) (Fig. 2B). Concurrently, *VEGF* expression was significantly higher in the 0.2, 0.5, 0.8, and 1.2 mM groups than that in the control group ($P < 0.05$) (Fig. 2D). However, *Bcl-2* expression was not significantly different in the 0.5, 0.8, and 1.2 mM groups compared with the 0.2 mM group ($P > 0.05$) (Fig. 2C).

Total protein was extracted from PAL treated cells and the expression of apoptotic proteins was analyzed. Results showed that the protein levels of caspase 3 and VEGF were enhanced after PAL stimulation (Fig. 2E). Grayscale analysis revealed no significant difference in caspase 3 expression between the 0.2 mM group and the control group ($P > 0.05$). However, caspase 3 expression was significantly enhanced in the 0.5, 0.8, and 1.2 mM groups compared to the control group ($P < 0.05$, $P < 0.01$, and $P < 0.001$, respectively). Furthermore, caspase 3 levels were significantly higher in the 0.5, 0.8, and 1.2 mM groups compared to the 0.2 mM group ($P < 0.05$, $P < 0.01$, and $P < 0.001$, respectively) (Fig. 2E, F). VEGF expression exhibited a similar tendency as caspase 3, but to a lower extent (Fig. 2E, G). A significant increase in VEGF expression was observed in the 0.8 and 1.2 mM groups compared with the control group ($P < 0.05$), while no significant difference was detected compared with the 0.2 mM group ($P > 0.05$). In conclusion, the expression of apoptosis related genes was enhanced in a dose-dependent way after PAL stimulation for 24 h.

4. Effects of different incubation times with palmitate on cell survival

Considering the optimal effects on gene expression and cell viability, based on the above results, a PAL concentration of 0.5 mM was chosen for subsequent experiments. To analyze the effects of different incubation times on cell injury and apoptosis, cells were divided into the 0, 4, 8, 16, 24, and 48 h groups, and cell viability at each time point was examined by MTT assay. Results showed that a significant difference was observed at 8 h compared to 0 h ($P < 0.05$). The cell viability at 16, 24, and 48 h was decreased significantly compared to the 0 h group ($P < 0.01$), and it was significantly decreased at 24 h and 48 h compared to the 8 h group ($P < 0.05$) (Fig. 3A).

5. PAL incubation time affected the expression of apoptosis related genes

Samples were collected at different time points to detect the expression of apoptosis related genes. The transcriptional expression of *CASP3* showed no statistical significance between 4 h and 0 h ($P > 0.05$). *CASP3* expression was significantly higher at 8 h ($P < 0.05$) and 16 h ($P < 0.01$) compared to 0 h; subsequently, the increase diminished. *CASP3* expression was significantly higher at 16, 24, and 48 h ($P < 0.05$) compared with the 8 h group (Fig. 3B). The expression of *Bcl-2*, an antiapoptotic gene, showed a slight increase at different time points, but no statistical difference was observed ($P > 0.05$) (Fig. 3C). The expression of *Bax*, a proapoptotic gene, showed no significant difference between 4 h and 0 h ($P > 0.05$). *Bax* expression at 8 h and 16 h was significantly higher compared to the control group ($P < 0.05$ and $P < 0.01$). *Bax* expression was significantly higher at 16, 24, and 48 h than at 4 h ($P < 0.05$) (Fig. 3D). *VEGF*

expression showed a time-dependent increasing trend; no significant difference was observed for the 4 and 8 h groups compared with the 0 h group ($P > 0.05$), while the expression at 16 h was significantly increased compared to the 0 h group ($P < 0.05$). At 24 and 48 h, *VEGF* expression was significantly higher than at 0 and 4 h, while no significant difference was observed compared to the 8 h group ($P > 0.05$) (Fig. 3E).

Total protein was extracted and the expression of apoptosis related factors was analysed by western blot analysis. With respect to caspase 3 expression, no significant difference was observed between the 4 h group and the 0 h group ($P > 0.05$), but after 8, 16, 24, and 48 h, caspase 3 expression was significantly higher than in the control group ($P < 0.05$, $P < 0.01$, $P < 0.01$, and $P < 0.001$, respectively). No significant difference was observed between the 8 h group and the 4 h group ($P > 0.05$), while expression of caspase 3 was significantly higher in the 16, 24, and 48 h groups compared to the 4 h group ($P < 0.01$) (Fig. 3F, G). VEGF protein expression also showed a time-dependent increasing trend. A significant increase was observed in the 4 h and 8 h groups compared to the 0 h group ($P < 0.05$), while no difference was observed between the 4 h group and the 8 h group ($P > 0.05$). At 16 h, VEGF expression was significantly higher than that in the 4 h and 8 h groups ($P < 0.01$). No significant difference in VEGF protein expression was observed among the 16, 24, and 48 h groups ($P > 0.05$) (Fig. 3F, H).

In summary, the apoptosis rate exhibited a time-dependent increase after PAL stimulation and the expression of apoptosis related genes and VEGF was enhanced.

6. VEGF overexpression ameliorated cell injury

Enhanced expression of VEGF hinted towards its role in the regulation of the apoptosis process. Therefore, a plasmid containing human *VEGFA* cDNA was constructed and administered to HHHM2 cells. Results showed that the expression of VEGFA was boosted at the transcriptional level (48 h, Fig. 4A) and the translational level (24 h, 48 h, Fig. 4B, C). Moreover, no significant difference in cell apoptosis rate was found by flow cytometry ($P > 0.05$) (Fig. 4D, E).

We then measured the expression levels of apoptosis related factors at 0, 24, and 48 h. The expression level of caspase 3, a key executor of the apoptotic pathway, was significantly decreased in the 24 h group ($P < 0.05$), and its expression level decreased significantly after 48 h incubation with PAL ($P < 0.01$) (Fig. 5A).

A similar decreasing trend was observed for caspase 3 protein expression at 24 h ($P < 0.05$) and 48 h ($P < 0.05$) (Fig. 5E, F). Compared with the control group, the expression level of the antiapoptotic factor Bcl-2 exhibited no significant difference in the 24 h group ($P > 0.05$), while it was significantly increased at 48 h ($P < 0.05$) (Fig. 5B). On the contrary, Bcl-2 protein expression was significantly higher than that of the control group at 24 h ($P < 0.05$) and 48 h ($P < 0.01$) (Fig. 5E, G).

Compared with the control group, expression of the proapoptotic factor *Bax* significantly decreased in the 24 h group ($P < 0.05$) and the 48 h group ($P < 0.01$) (Fig. 5C). Bax protein expression declined at 24 h ($P < 0.05$) and 48 h ($P < 0.01$) (Fig. 5E, H). Expression of *p65*, encoding a subunit of the NF-κB transcriptional

complex, was significantly decreased at 24 h ($P < 0.05$) and 48 h ($P < 0.01$) compared with the control group (Fig. 5D). Meanwhile, p65 protein expression was significantly lower at 24 h ($P < 0.05$) and 48 h ($P < 0.01$) (Fig. 5E, I).

In summary, VEGFA overexpression increased the cell survival rate and reduced the apoptosis rate after PAL incubation, and VEGFA overexpression significantly lowered the expression of apoptosis related factors.

7. The JNK pathway, but not the ERK pathway, functioned in VEGF regulated cell apoptosis

Studies have shown that the c-Jun N-terminal protein kinase (JNK) and ERK pathways play important regulatory roles in the process of apoptosis. Therefore, we detected the protein expression of both. The expression level of phosphorylated JNK (p-JNK) was significantly lower in the 24 h and 48 h groups than in the control group ($P < 0.05$) (Fig. 6A, B); no significant difference was observed in the JNK protein level at 24 and 48 h ($P > 0.05$) (Fig. 6A, B). However, the expression level of phosphorylated ERK (p-ERK) was not significantly different in the 24 and 48 h groups ($P > 0.05$) (Fig. 6C, D), and there was no significant difference in total ERK protein expression between the 24 h and 48 h groups ($P > 0.05$) (Fig. 6C, D).

After HHHM2 cells were transfected with VEGFA plasmid and control cells were transfected with empty vector, cells were incubated with 0.5 mM PAL for different periods of time and caspase 3 activity was evaluated with the caspase 3 activity assay kit. The results showed that caspase 3 activity in the 12 h group was significantly lower than that in the control group ($P < 0.05$), and caspase 3 activity in the 24 and 48 h groups was significantly lower than that in the control group ($P < 0.01$) (Fig. 6E).

Discussion

Cardiovascular disease has become the number one challenge endangering human health in today's society according to the World Health Organization (27). The age-adjusted prevalence of total heart diseases is 10.6% based on the 2017 National Health Interview Survey, and the prevalence is 11.0%, 9.7%, 7.4%, and 6.1% among whites, blacks, Hispanics, and Asians, respectively (28). Statistics from the United States show that in 2018, about 163.6 people per 100,000 standard population died of heart disease, making heart disease the leading cause of death (29,30). In the present study, an in vitro model of lipotoxicity induced cell injury was successfully constructed. After incubation with 0.5 mM PAL for 24 h, cell viability was significantly reduced, apoptosis was upregulated, and VEGF expression was increased. After transient transfection with VEGF, VEGF overexpression ameliorated lipotoxicity induced cell injury and lowered the activity of JNK.

Ectopically deposited fatty acids in the heart result in lipotoxicity, injury to cardiomyocytes, and myocardial apoptosis (3). PAL, also known as hexadecane, is a commonly consumed saturated fatty acid. Numerous studies have reported that PAL induced apoptosis in a variety of cells, including Chinese hamster ovary (CHO) cells, rat islet cells, retinal microvascular endothelial cells, and myocardial cells

(31–34). A review of the published literature shows that mitochondrial pathways, death receptor pathways, and endoplasmic reticulum pathways are involved in the PAL induced apoptotic process (35,36). Overstimulation by PAL causes irreversible alteration of mitochondrial permeability and osmotic pressure, thus inducing caspase 9 to activate caspase 3 and caspase 7 to cleave downstream substrates (37). In addition, Bcl-2 family members play an important role in regulating mitochondrial membrane permeability. Bcl-xl and Bcl-2 are distributed the in mitochondrial membrane and the cytoplasm, whereas Bax and Bid are located in the cytoplasm (38). Mitochondrial damage leads to loss of normal morphology and energy metabolism (39). Many questions on the relationship between VEGF and PAL in cardiomyocyte apoptosis still remain to be answered. In the present study, the effects of different concentrations and incubation times of PAL on apoptosis in HHHM2 cells were determined by cell viability assays and analysis of the expression of apoptotic factors. Cells were cultured with medium containing 0.2, 0.5, 0.8, and 1.2 mM PAL for 24 h to determine the optimal PAL concentration to induce the cell injury model. Furthermore, different incubation times (0, 4, 8, 16, 24, and 48 h) were adopted to screen the appropriate time for the cell injury model construction. In addition, we also detected the levels of the antiapoptotic Bcl-2 and the proapoptotic Bax, as well as the downstream protein caspase 3. Results showed that PAL increased Bax and caspase 3 levels, while it decreased the expression of VEGF, thus promoting cell apoptosis.

VEGF was reported as a vital factor in the promotion of angiogenesis by inhibiting endothelial cell apoptosis upon PAL treatment (40,41). In the present study, we focused on cell survival and apoptosis during PAL incubation to investigate the role of VEGF in cardiomyocytes. Since incubation with PAL boosted the expression of VEGF, we hypothesized that VEGF might play a pivotal role in lipotoxicity induced myocardial apoptosis. 12-Deoxyphorbol 13-palmitate was reported to inhibit the expression of VEGF in MCF-7 cells, which was inconsistent with the results in the present study, possibly because different cells were used in different studies. Next, VEGF was overexpressed and the effects of VEGF on normal and PAL treated HHHM2 cells were evaluated. The PAL induced decrease in cell viability was ameliorated by VEGF overexpression by inhibiting Bax and caspase 3 expression, while enhancing Bcl-2 expression.

The JNK/ERK signaling pathway has been reported to be involved in apoptosis. Previous reports indicated that a high fat diet induced activation of JNK, which was reversed by *TLR4* knockout (42). Cellular accumulation of ceramide activated JNK signaling and apoptosis, which was prevented by ceramide synthase 5 (*CERS5*) knockdown (43). JNK activation was observed in PAL treated cardiomyocytes and attenuated by protein kinase R (PKR) inhibition (44). In the present study, we analyzed the expression of proteins involved in the JNK and ERK pathways in cells overexpressing VEGF after PAL treatment. JNK activity was enhanced after PAL incubation, which was alleviated after VEGF overexpression. However, no significant variation in ERK levels was detected. The results suggest a novel role of VEGF in antagonizing cytotoxicity in cardiomyocytes, indicating a potential therapeutic strategy for cardiac protection.

Abbreviations

PAL palmitate

VEGF Vascular endothelial growth factor

PDGF Platelet-derived growth factors

ERK Extracellular signal regulated kinase

JNK c-Jun N-terminal kinase

PI Propidium iodide

Declarations

Ethics approval and consent to participate

Not applicable.

Consent for publication

Not applicable.

Availability of data and materials

The datasets used and/or analysed during the current study available from the corresponding author on reasonable request.

Competing interests

We declare that no other IRB approval was required in this study. And we have no financial and personal relationships with other people or organizations that can inappropriately influence our work. There was no competing interest. All authors have participated in our research. And the article has not been published elsewhere. Funding

This work was financially supported by the The Priority Academic Program Development (PAPD) of Jiangsu Higher Education Institutions; Jiangsu Government Scholarship for Overseas Studies (JS-2017-200). Project of Nantong Science and Technology Bureau (MS12018041, MS12018020).

Authors' contributions

SW and XL conceived and designed the study. SW, CZ, and QW performed the experiments. QW provided the cells transfected with VEGFA plasmid. SW, XL, SG and YY wrote the paper. XL, YY, SG and XL reviewed and edited the manuscript. All authors read and approved the manuscript.

Acknowledgements

We appreciated Dr. Qingquan Zhang for generously gifting us the VEGFA plasmids.

References

1. Heallen, T. R., Kadow, Z. A., Kim, J. H., Wang, J., and Martin, J. F. (2019) Stimulating Cardiogenesis as a Treatment for Heart Failure. *Circulation research* **124**, 1647-1657
2. Nasser, M. I., Qi, X., Zhu, S., He, Y., Zhao, M., Guo, H., and Zhu, P. (2020) Current situation and future of stem cells in cardiovascular medicine. *Biomed Pharmacother* **132**, 110813
3. Li, X., Wu, Y., Zhao, J., Wang, H., Tan, J., Yang, M., Li, Y., Deng, S., Gao, S., Li, H., Yang, Z., Yang, F., Ma, J., Cheng, J., and Cai, W. (2020) Distinct cardiac energy metabolism and oxidative stress adaptations between obese and non-obese type 2 diabetes mellitus. *Theranostics* **10**, 2675-2695
4. Lin, Y. H., Kang, L., Feng, W. H., Cheng, T. L., Tsai, W. C., Huang, H. T., Lee, H. C., and Chen, C. H. (2020) Effects of Lipids and Lipoproteins on Mesenchymal Stem Cells Used in Cardiac Tissue Regeneration. *Int J Mol Sci* **21**
5. Cacicedo, J. M., Benjachareowong, S., Chou, E., Ruderman, N. B., and Ido, Y. (2005) Palmitate-induced apoptosis in cultured bovine retinal pericytes: roles of NAD(P)H oxidase, oxidant stress, and ceramide. *Diabetes* **54**, 1838-1845
6. Zhou, X., Li, Z., Qi, M., Zhao, P., Duan, Y., Yang, G., and Yuan, L. (2020) Brown adipose tissue-derived exosomes mitigate the metabolic syndrome in high fat diet mice. *Theranostics* **10**, 8197-8210
7. Puzyrenko, A. M., Chekman, I. S., Briuzhina, T. S., and Horchakova, N. O. (2013) [Influence of antihypertensive and metabolic drugs on fatty acids content of lipids in cardiomyocytes of rats with spontaneous hypertension]. *Ukr Biokhim Zh (1999)* **85**, 67-74
8. Chai, W., and Liu, Z. (2007) p38 mitogen-activated protein kinase mediates palmitate-induced apoptosis but not inhibitor of nuclear factor-kappaB degradation in human coronary artery endothelial cells. *Endocrinology* **148**, 1622-1628
9. Quan, J., Liu, J., Gao, X., Liu, J., Yang, H., Chen, W., Li, W., Li, Y., Yang, W., and Wang, B. (2014) Palmitate induces interleukin-8 expression in human aortic vascular smooth muscle cells via Toll-like receptor 4/nuclear factor-kappaB pathway (TLR4/NF-kappaB-8). *J Diabetes* **6**, 33-41
10. Gorgani-Firuzjaee, S., Ahmadi, S., and Meshkani, R. (2014) Palmitate induces SHIP2 expression via the ceramide-mediated activation of NF-kappaB, and JNK in skeletal muscle cells. *Biochemical and biophysical research communications* **450**, 494-499

11. Le, Y., Wei, R., Yang, K., Lang, S., Gu, L., Liu, J., Hong, T., and Yang, J. (2020) Liraglutide ameliorates palmitate-induced oxidative injury in islet microvascular endothelial cells through GLP-1 receptor/PKA and GTPCH1/eNOS signaling pathways. *Peptides* **124**, 170212
12. Geng, Y., Hernandez Villanueva, A., Oun, A., Buist-Homan, M., Blokzijl, H., Faber, K. N., Dolga, A., and Moshage, H. (2020) Protective effect of metformin against palmitate-induced hepatic cell death. *Biochim Biophys Acta Mol Basis Dis* **1866**, 165621
13. Xiong, Z., Li, Y., Zhao, Z., Zhang, Y., Man, W., Lin, J., Dong, Y., Liu, L., Wang, B., Wang, H., Guo, B., Li, C., Li, F., Wang, H., and Sun, D. (2020) Mst1 knockdown alleviates cardiac lipotoxicity and inhibits the development of diabetic cardiomyopathy in db/db mice. *Biochim Biophys Acta Mol Basis Dis* **1866**, 165806
14. Tong, M., Saito, T., Zhai, P., Oka, S. I., Mizushima, W., Nakamura, M., Ikeda, S., Shirakabe, A., and Sadoshima, J. (2019) Mitophagy Is Essential for Maintaining Cardiac Function During High Fat Diet-Induced Diabetic Cardiomyopathy. *Circulation research* **124**, 1360-1371
15. Kenny, H. C., and Abel, E. D. (2019) Heart Failure in Type 2 Diabetes Mellitus. *Circulation research* **124**, 121-141
16. Chiu, H. C., Kovacs, A., Blanton, R. M., Han, X., Courtois, M., Weinheimer, C. J., Yamada, K. A., Brunet, S., Xu, H., Nerbonne, J. M., Welch, M. J., Fettig, N. M., Sharp, T. L., Sambandam, N., Olson, K. M., Ory, D. S., and Schaffer, J. E. (2005) Transgenic expression of fatty acid transport protein 1 in the heart causes lipotoxic cardiomyopathy. *Circulation research* **96**, 225-233
17. Cheng, L., Ding, G., Qin, Q., Huang, Y., Lewis, W., He, N., Evans, R. M., Schneider, M. D., Brako, F. A., Xiao, Y., Chen, Y. E., and Yang, Q. (2004) Cardiomyocyte-restricted peroxisome proliferator-activated receptor-delta deletion perturbs myocardial fatty acid oxidation and leads to cardiomyopathy. *Nature medicine* **10**, 1245-1250
18. Li, D., Xie, K., Zhang, L., Yao, X., Li, H., Xu, Q., Wang, X., Jiang, J., and Fang, J. (2016) Dual blockade of vascular endothelial growth factor (VEGF) and basic fibroblast growth factor (FGF-2) exhibits potent anti-angiogenic effects. *Cancer Lett* **377**, 164-173
19. Ferrara, N. (2004) Vascular endothelial growth factor: basic science and clinical progress. *Endocr Rev* **25**, 581-611
20. Ho, Q. T., and Kuo, C. J. (2007) Vascular endothelial growth factor: biology and therapeutic applications. *Int J Biochem Cell Biol* **39**, 1349-1357
21. Oka, T., Akazawa, H., Naito, A. T., and Komuro, I. (2014) Angiogenesis and cardiac hypertrophy: maintenance of cardiac function and causative roles in heart failure. *Circulation research* **114**, 565-571
22. Bowers, S. L. K., Kemp, S. S., Aguera, K. N., Koller, G. M., Forgy, J. C., and Davis, G. E. (2020) Defining an Upstream VEGF (Vascular Endothelial Growth Factor) Priming Signature for Downstream Factor-Induced Endothelial Cell-Pericyte Tube Network Coassembly. *Arterioscler Thromb Vasc Biol*, ATVBAHA120314517

23. Harper, S. J., and Bates, D. O. (2008) VEGF-A splicing: the key to anti-angiogenic therapeutics? *Nat Rev Cancer* **8**, 880-887
24. Rennel, E. S., Hamdollah-Zadeh, M. A., Wheatley, E. R., Magnussen, A., Schuler, Y., Kelly, S. P., Finucane, C., Ellison, D., Cebe-Suarez, S., Ballmer-Hofer, K., Mather, S., Stewart, L., Bates, D. O., and Harper, S. J. (2008) Recombinant human VEGF165b protein is an effective anti-cancer agent in mice. *Eur J Cancer* **44**, 1883-1894
25. Huang, J. B., Hsu, S. P., Pan, H. Y., Chen, S. D., Chen, S. F., Lin, T. K., Liu, X. P., Li, J. H., Chen, N. C., Liou, C. W., Hsu, C. Y., Chuang, H. Y., and Chuang, Y. C. (2020) Peroxisome Proliferator-Activated Receptor gamma Coactivator 1alpha Activates Vascular Endothelial Growth Factor That Protects Against Neuronal Cell Death Following Status Epilepticus through PI3K/AKT and MEK/ERK Signaling. *Int J Mol Sci* **21**
26. Song, M., and Finley, S. D. (2020) ERK and Akt exhibit distinct signaling responses following stimulation by pro-angiogenic factors. *Cell Commun Signal* **18**, 114
27. Rodriguez, C. J., Allison, M., Daviglus, M. L., Isasi, C. R., Keller, C., Leira, E. C., Palaniappan, L., Pina, I. L., Ramirez, S. M., Rodriguez, B., Sims, M., American Heart Association Council on, E., Prevention, American Heart Association Council on Clinical, C., American Heart Association Council on, C., and Stroke, N. (2014) Status of cardiovascular disease and stroke in Hispanics/Latinos in the United States: a science advisory from the American Heart Association. *Circulation* **130**, 593-625
28. Virani, S. S., Alonso, A., Benjamin, E. J., Bittencourt, M. S., Callaway, C. W., Carson, A. P., Chamberlain, A. M., Chang, A. R., Cheng, S., Delling, F. N., Djousse, L., Elkind, M. S. V., Ferguson, J. F., Fornage, M., Khan, S. S., Kissela, B. M., Knutson, K. L., Kwan, T. W., Lackland, D. T., Lewis, T. T., Lichtman, J. H., Longenecker, C. T., Loop, M. S., Lutsey, P. L., Martin, S. S., Matsushita, K., Moran, A. E., Mussolino, M. E., Perak, A. M., Rosamond, W. D., Roth, G. A., Sampson, U. K. A., Satou, G. M., Schroeder, E. B., Shah, S. H., Shay, C. M., Spartano, N. L., Stokes, A., Tirschwell, D. L., VanWagner, L. B., Tsao, C. W., American Heart Association Council on, E., Prevention Statistics, C., and Stroke Statistics, S. (2020) Heart Disease and Stroke Statistics-2020 Update: A Report From the American Heart Association. *Circulation* **141**, e139-e596
29. Xu, J., Murphy, S. L., Kockanek, K. D., and Arias, E. (2020) Mortality in the United States, 2018. *NCHS Data Brief*, 1-8
30. Xu, J., Murphy, S. L., Kochanek, K. D., and Arias, E. (2020) Mortality in the United States, 2018. *National Vital Statistics Reports* **355**, 7
31. Listenberger, L. L., Ory, D. S., and Schaffer, J. E. (2001) Palmitate-induced apoptosis can occur through a ceramide-independent pathway. *The Journal of biological chemistry* **276**, 14890-14895
32. Lytrivi, M., Castell, A. L., Poitout, V., and Cnop, M. (2020) Recent Insights Into Mechanisms of beta-Cell Lipo- and Glucolipotoxicity in Type 2 Diabetes. *J Mol Biol* **432**, 1514-1534
33. Yamagishi, S., Okamoto, T., Amano, S., Inagaki, Y., Koga, K., Koga, M., Choei, H., Sasaki, N., Kikuchi, S., Takeuchi, M., and Makita, Z. (2002) Palmitate-induced apoptosis of microvascular endothelial cells and pericytes. *Mol Med* **8**, 179-184

34. Sparagna, G. C., Hickson-Bick, D. L., Buja, L. M., and McMillin, J. B. (2000) A metabolic role for mitochondria in palmitate-induced cardiac myocyte apoptosis. *Am J Physiol Heart Circ Physiol* **279**, H2124-2132
35. Westermann, B. (2010) Mitochondrial fusion and fission in cell life and death. *Nat Rev Mol Cell Biol* **11**, 872-884
36. Vakifahmetoglu-Norberg, H., Ouchida, A. T., and Norberg, E. (2017) The role of mitochondria in metabolism and cell death. *Biochemical and biophysical research communications* **482**, 426-431
37. Pradelli, L. A., Beneteau, M., and Ricci, J. E. (2010) Mitochondrial control of caspase-dependent and -independent cell death. *Cell Mol Life Sci* **67**, 1589-1597
38. Czabotar, P. E., Lessene, G., Strasser, A., and Adams, J. M. (2014) Control of apoptosis by the BCL-2 protein family: implications for physiology and therapy. *Nat Rev Mol Cell Biol* **15**, 49-63
39. Richter, C., Schweizer, M., Cossarizza, A., and Franceschi, C. (1996) Control of apoptosis by the cellular ATP level. *FEBS Lett* **378**, 107-110
40. Yang, Y., Cong, H., Han, C., Yue, L., Dong, H., and Liu, J. (2015) 12-Deoxyphorbol 13-palmitate inhibits the expression of VEGF and HIF-1alpha in MCF-7 cells by blocking the PI3K/Akt/mTOR signaling pathway. *Oncology reports* **34**, 1755-1760
41. Xu, T., Lv, Z., Chen, Q., Guo, M., Wang, X., and Huang, F. (2018) Vascular endothelial growth factor over-expressed mesenchymal stem cells-conditioned media ameliorate palmitate-induced diabetic endothelial dysfunction through PI-3K/AKT/m-TOR/eNOS and p38/MAPK signaling pathway. *Biomed Pharmacother* **106**, 491-498
42. Hu, N., and Zhang, Y. (2017) TLR4 knockout attenuated high fat diet-induced cardiac dysfunction via NF-kappaB/JNK-dependent activation of autophagy. *Biochim Biophys Acta Mol Basis Dis* **1863**, 2001-2011
43. Leonardini, A., D'Oria, R., Incalza, M. A., Caccioppoli, C., Andrulli Buccheri, V., Cignarelli, A., Paparella, D., Margari, V., Natalicchio, A., Perrini, S., Giorgino, F., and Laviola, L. (2017) GLP-1 Receptor Activation Inhibits Palmitate-Induced Apoptosis via Ceramide in Human Cardiac Progenitor Cells. *J Clin Endocrinol Metab* **102**, 4136-4147
44. Mangali, S., Bhat, A., Udumula, M. P., Dhar, I., Sriram, D., and Dhar, A. (2019) Inhibition of protein kinase R protects against palmitic acid-induced inflammation, oxidative stress, and apoptosis through the JNK/NF-kB/NLRP3 pathway in cultured H9C2 cardiomyocytes. *J Cell Biochem* **120**, 3651-3663

Figures

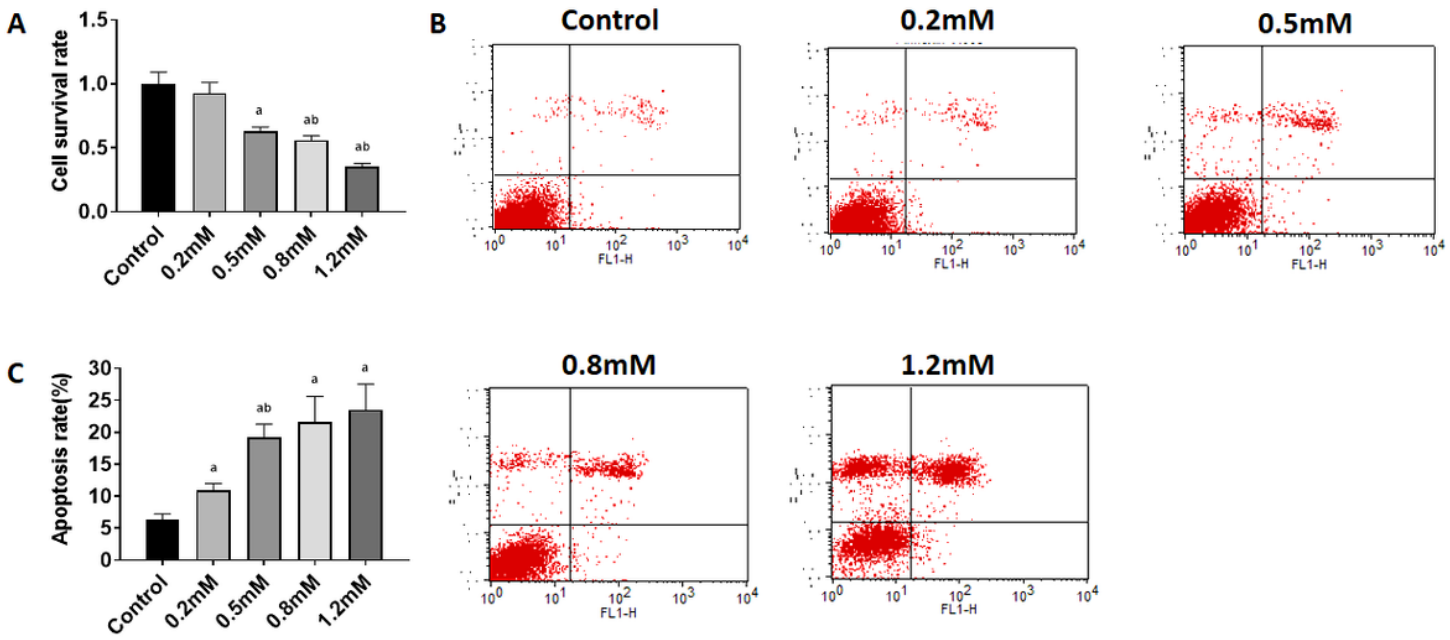

Figure 1

Cell survival and apoptosis after treatment with different PAL concentrations. A. Cell survival rate. B. Flow cytometry analysis of PAL treated HHHM2 cells. C. Statistical analysis of the flow cytometry results. a, $P < 0.05$ compared with the control group; b, $P < 0.05$ compared with the 0.2 mM group. n = 7 for cell survival investigation and n = 3 for FACs analysis.

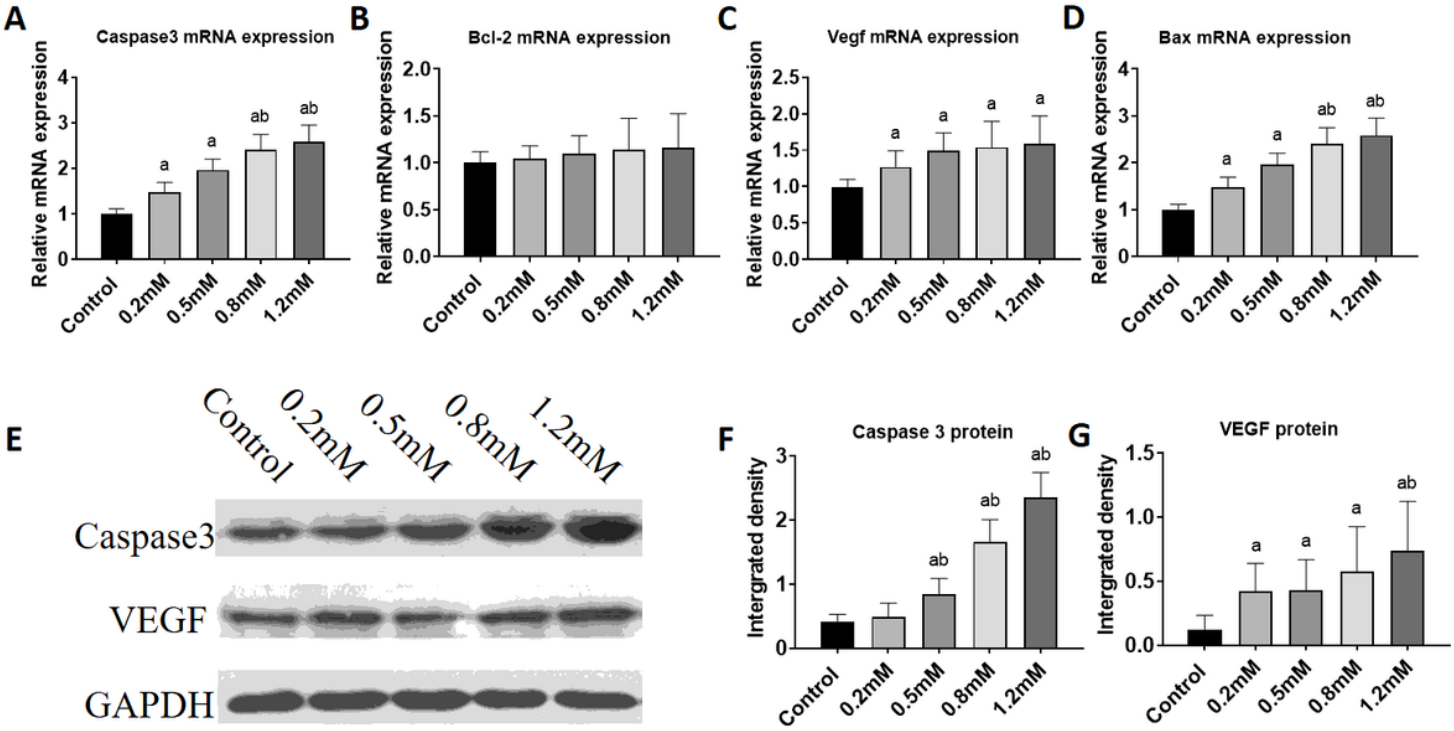

Figure 2

Expression of apoptosis related genes after treatment with different concentrations of PAL. A. CASP3 mRNA expression. B. Bax mRNA expression. C. Bcl-2 mRNA expression. D. VEGF mRNA expression. E. Western blot analysis of caspase 3 and VEGF. F. Grayscale analysis for caspase 3. G. Grayscale analysis for VEGF. a, P < 0.05 compared with the control group; b, P < 0.05 compared with the 0.2 mM group. n = 8 for mRNA detection and n = 3 for blots.

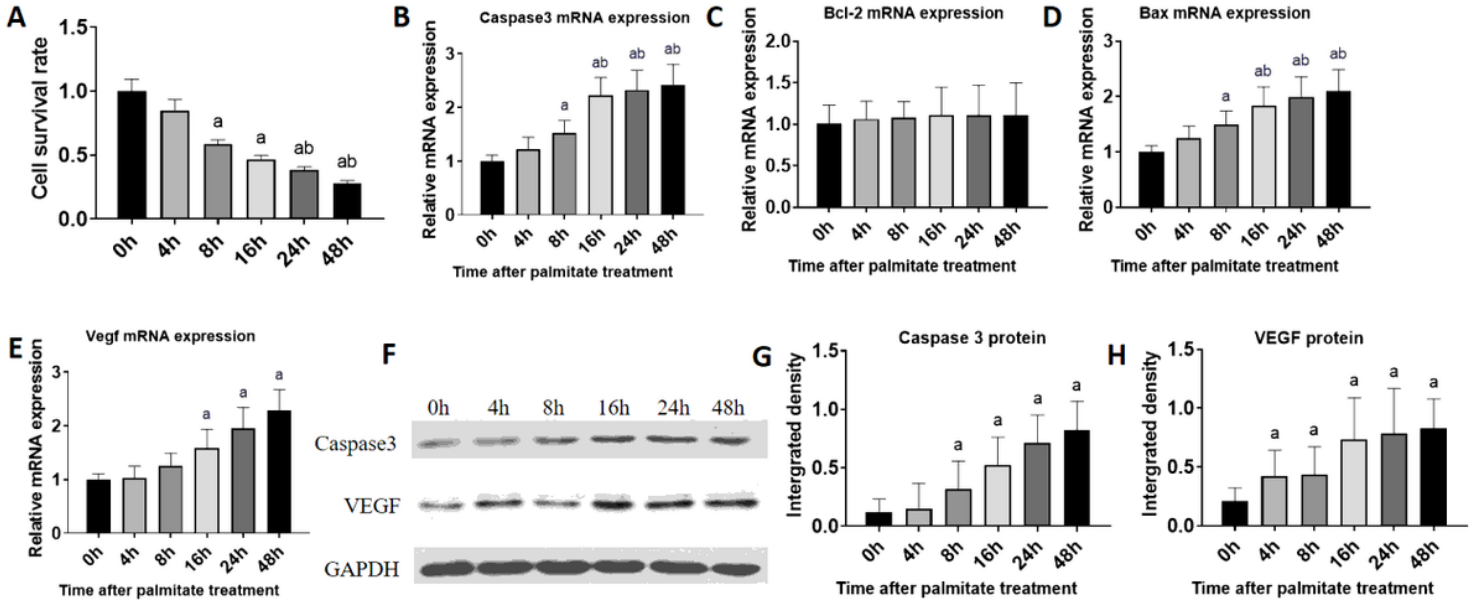

Figure 3

Incubation time of cardiomyocytes with PAL influenced cell survival and the expression of apoptotic genes. A. Cell survival rate. B. CASP3 mRNA expression. C. Bcl-2 mRNA expression. D. Bax mRNA expression. E. VEGF mRNA expression. F. Western blot analysis of the expression of caspase 3 and VEGF. G. Grayscale analysis for caspase 3. H. Grayscale analysis for VEGF. . a, P < 0.05 compared with the control group; b, P < 0.05 compared with the 0.2 mM group. n = 8 for mRNA detection and n = 3 for blots.

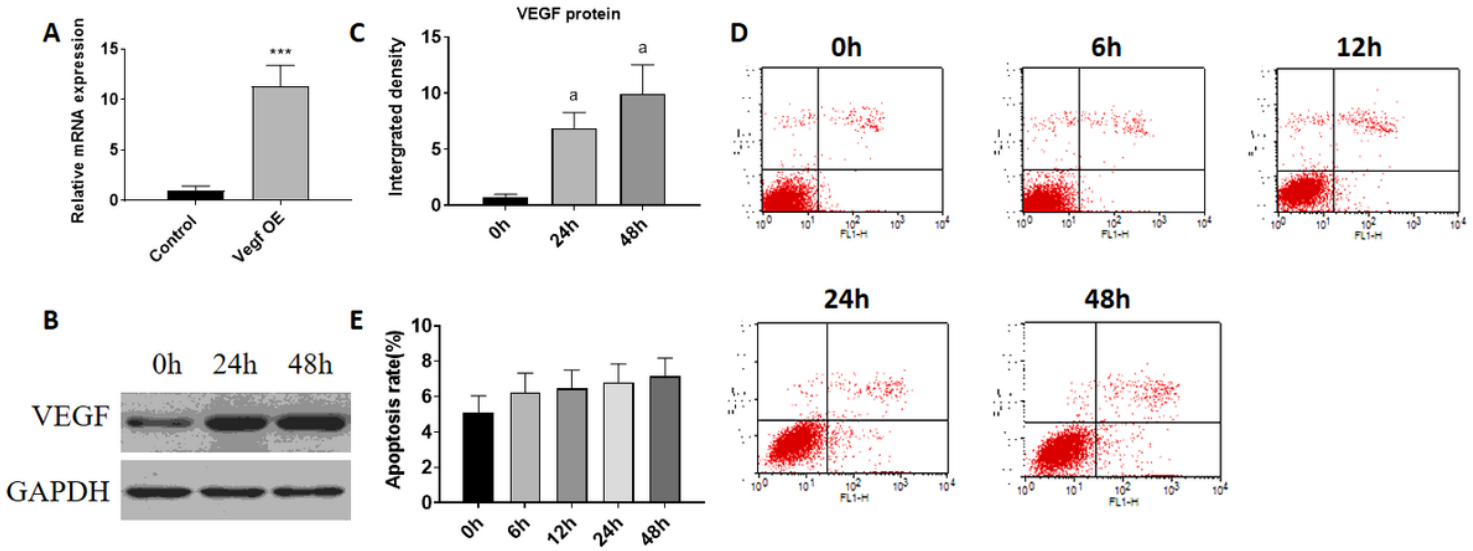

Figure 4

VEGF overexpression reduced the apoptotic effects of PAL. A. VEGF mRNA expression after exotic transfection. B. Western blot analysis of VEGF. C. Grayscale analysis for VEGF. D. Flow cytometry analysis of the apoptosis of cardiomyocytes. E. Statistical analysis of FACS results. a, P < 0.05 compared with the control group. n =3.

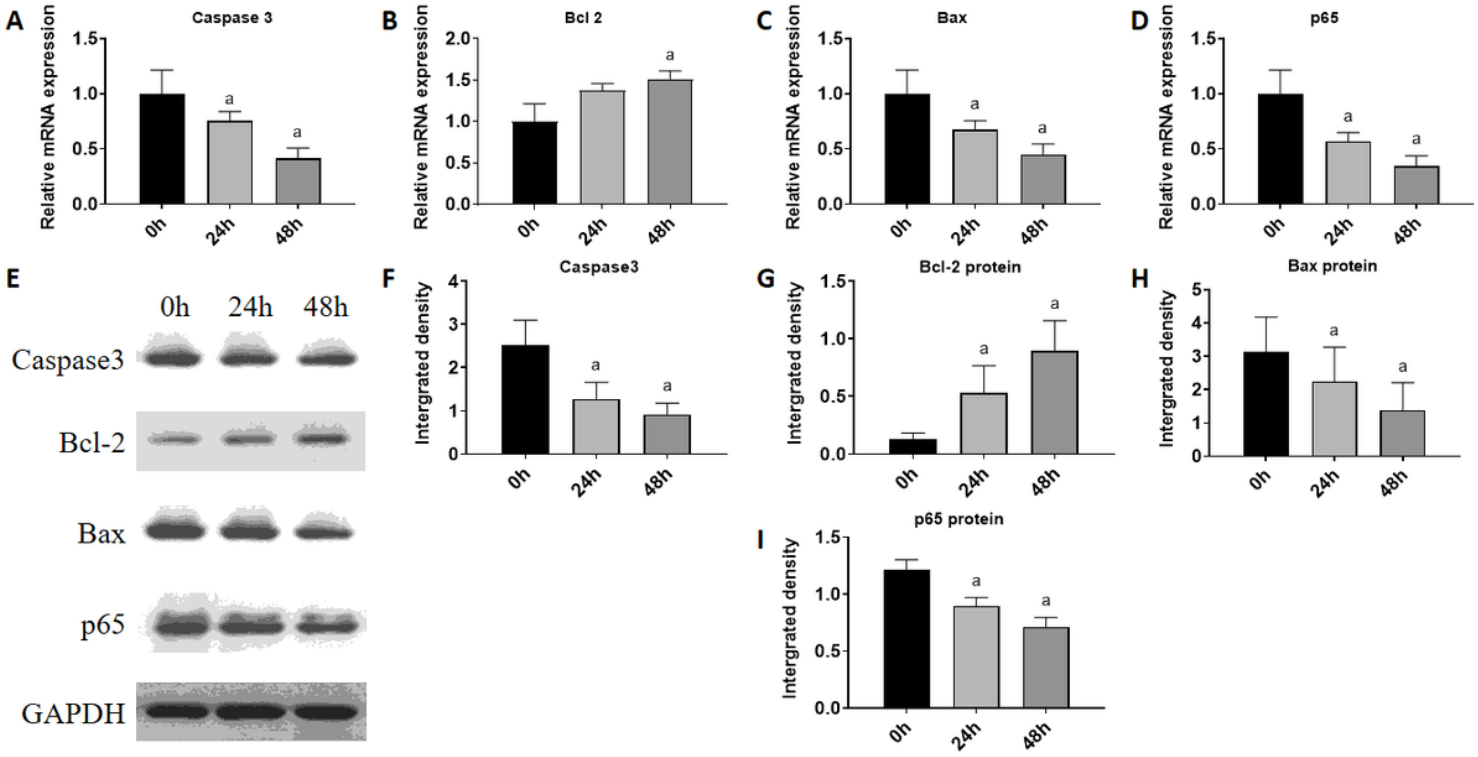

Figure 5

VEGF overexpression reversed the apoptosis of cardiomyocytes. A-D. Transcriptional changes of CASP3, Bcl-2, Bax, and p65 after VEGF overexpression in PAL incubated cardiomyocytes. E. Protein expression of Caspase 3, Bcl-2, Bax, and p65. F-I. Grayscale analysis for Caspase 3, Bcl-2, Bax, and p65 in figure 5E. a, P < 0.05 compared with the control group. n = 8 for mRNA detection and n = 3 for blots.

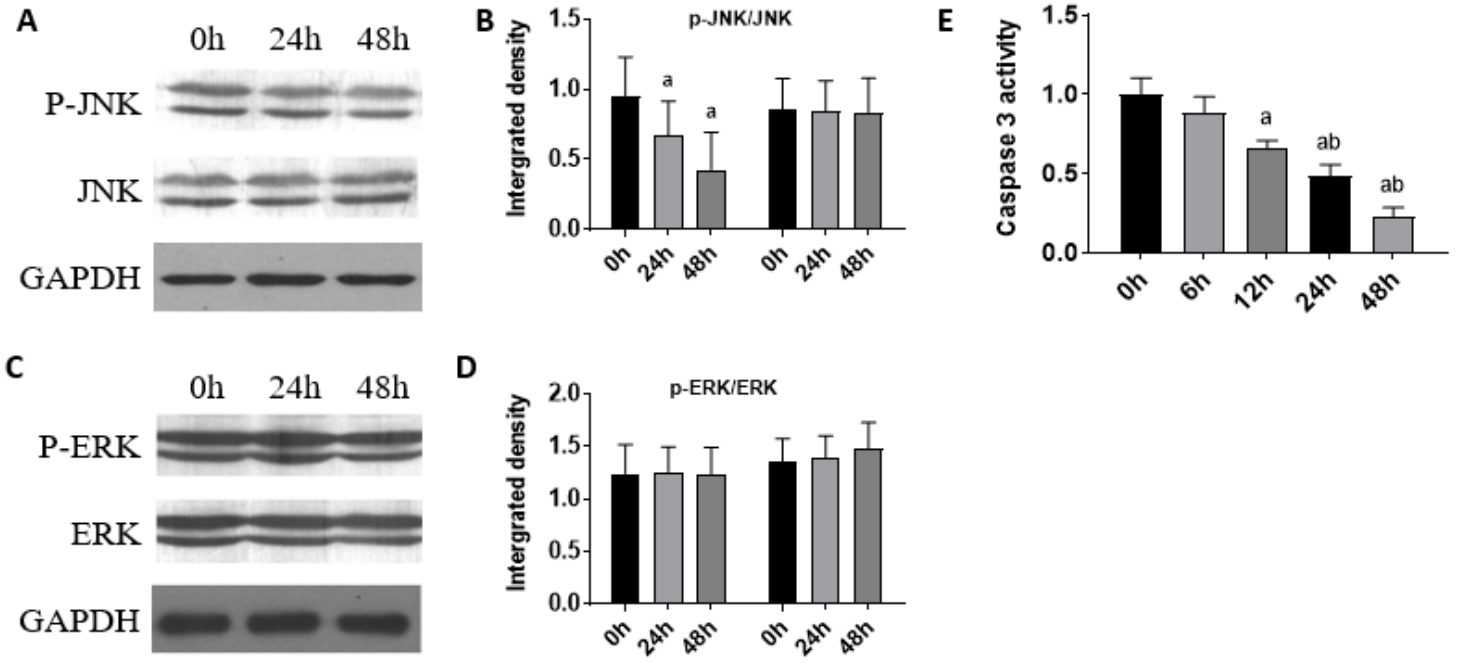

Figure 6

Variation of the JNK and ERK pathways under condition of VEGF oeverexpression. A. Protein levels of p-JNK and JNK. B. Grayscale analysis for p-JNK and JNK. C. Protein levels of p-ERK and ERK. D. Grayscale analysis for p-ERK and ERK. E. Enzyme activity of Caspase 3. a, $P < 0.05$ compared with the control group. b, $P < 0.05$ compared with the 0.2 mM group. n = 3 for blots and n = 55 for enzyme activity analysis.